

See discussions, stats, and author profiles for this publication at: <https://www.researchgate.net/publication/14205643>

Progress Curve Analysis of the Kinetics with Which Blood Coagulation Factor XIa Is Inhibited by Protease Nexin-2 †

ARTICLE in BIOCHEMISTRY · JANUARY 1997

Impact Factor: 3.02 · DOI: 10.1021/bi9612576 · Source: PubMed

CITATIONS

34

READS

27

4 AUTHORS, INCLUDING:



Joseph Michael Scandura

Weill Cornell Medical College

39 PUBLICATIONS 991 CITATIONS

SEE PROFILE



William E Van Nostrand

Stony Brook University

157 PUBLICATIONS 6,703 CITATIONS

SEE PROFILE



Peter N Walsh

Temple University

173 PUBLICATIONS 4,876 CITATIONS

SEE PROFILE

Progress Curve Analysis of the Kinetics with Which Blood Coagulation Factor XIa Is Inhibited by Protease Nexin-2[†]

Joseph M. Scandura,^{‡,§} Yan Zhang,[‡] William E. Van Nostrand,[‡] and Peter N. Walsh^{*,†,§,||}

The Sol Sherry Thrombosis Research Center, Department of Biochemistry, Department of Medicine, Temple University School of Medicine, Philadelphia, Pennsylvania 19140, and Department of Medicine, HSC T-15/081, State University of New York, Stony Brook, New York 11794-8153

Received May 28, 1996; Revised Manuscript Received October 17, 1996[®]

ABSTRACT: Protease nexin-2 (PN-2), a soluble form of amyloid β -protein precursor (APP) containing a Kunitz protease inhibitor domain, has been shown to be a potent, reversible and competitive inhibitor of blood coagulation factor XIa (FXIa). We have analyzed progress curves of the hydrolysis of a sensitive fluorogenic substrate by FXIa in the presence of PN-2 to ascertain the kinetic rate constants governing the inhibition of FXIa by PN-2. The mechanism of this inhibition is best described as a slow equilibration between the free enzyme and inhibitor directly, without prior formation of a loosely-associated complex. The association rate constant (k_{on}) and the dissociation rate constant (k_{off}) were found to be $2.1 \pm 0.2 \times 10^6 \text{ M}^{-1} \text{ s}^{-1}$ and $8.5 \pm 0.8 \times 10^{-4} \text{ s}^{-1}$, respectively ($n = 23$). The inhibition constant calculated from these parameters (K_i) is 400 pM, in good agreement with previous reports. High molecular weight kininogen (HK) and Zn^{2+} ions exert opposite effects on the inhibition of FXIa by PN-2. HK protects FXIa from inactivation in a dose dependent and saturable manner ($\text{EC}_{50} = 61 \text{ nM}$) whereas Zn^{2+} augments the ability of PN-2 to inhibit FXIa. When both Zn^{2+} ions and HK are present, only the accessory effect of Zn^{2+} is observed. PN-2 is known to be an abundant platelet α -granule protein (Van Nostrand et al., 1990a; Smith & Broze, 1992). We conducted sensitive measurements of FXIa activity in the presence of human platelets before and after their being activated with the thrombin receptor agonist peptide, SFLLRN-amide. We found that platelet activation, and ostensibly the release of PN-2, limits the lifetime of FXIa activity within the locus of activated platelets. As in the purified system, HK protects FXIa from inactivation and Zn^{2+} increases the inactivation of FXIa. However, when HK and Zn^{2+} are both present, it is the protective effect of HK which predominates and prolongs the lifetime of FXIa after platelet activation.

Protease nexin-2 (PN-2)¹ is a secreted isoform of the precursor to the amyloid β -protein (i.e., amyloid β -protein precursor or APP) (Oltersdorf et al., 1989; Van Nostrand et

al., 1989) found in the neuritic plaques and cerebrovascular deposits of patients with Alzheimer's disease (Adams & Victor, 1993). This ~120 kDa soluble fragment of APP contains a Kunitz protease inhibitor domain (56 amino acids) encoded by exon 7 of the APP gene on chromosome 21 (Ponte et al., 1988; Tanzi et al., 1988; Kitaguchi et al., 1988). PN-2 is an abundant platelet α -granule protein which is secreted when platelets are stimulated by physiological agonists (Gardella et al., 1990, 1992, 1994; Li et al., 1994; Smith & Broze, 1992; Bush et al., 1990; Smith et al., 1990; Van Nostrand et al., 1990a). PN-2 accounts for roughly 0.5% of total platelet protein and virtually all (i.e., 99%) intravascular PN-2 circulates as a platelet component (Van Nostrand et al., 1991; Li et al., 1994).

PN-2 is a slow, tight-binding inhibitor of FXIa (Smith et al., 1990; Van Nostrand et al., 1990b); a form of inhibition common to members of the Kunitz protease inhibitor family (Salvesen & Pizzo, 1994). Platelets, cells which continually survey the lumen of blood vessels probing for sites of defect, represent a vehicle by which large quantities of PN-2 can be discharged into a nascent thrombus. For these reasons,

[†]Supported by Grants to P.N.W. from the National Institutes of Health (HL45486, HL25661, HL46213, and HL56153) and from the W. W. Smith Charitable Trust; to W.E.V.N. from the National Institutes of Health (HL49566 and a Research Career Development Award HL03229); and to J.M.S. from the Temple University M.D./Ph.D. Program.

* Author to whom correspondence should be addressed at the Sol Sherry Thrombosis Research Center, Temple University School of Medicine, 3400 North Broad Street, Philadelphia, PA 19140. Tel: (215) 707-4375. FAX: (215) 707-3005. E-mail: pnw@astro.ocis.temple.edu.

[‡] The Sol Sherry Thrombosis Research Center, Temple University School of Medicine.

[§] Department of Biochemistry, Temple University School of Medicine.

^{||} Department of Medicine, State University of New York.

[®] Department of Medicine, Temple University School of Medicine.

[®] Abstract published in *Advance ACS Abstracts*, December 15, 1996.

¹ Abbreviations used: PN-2, protease nexin-2; APP, amyloid β -protein precursor; FXIa, activated factor XI; HK, high molecular weight kininogen; HEPES, 4-(2-hydroxyethyl)-1-piperazineethanesulfonic acid; HBS, HEPES-buffered saline (135 mM NaCl, 15 mM HEPES, pH 7.4 at 37 °C); SFLLRN-amide, Ser-Phe-Leu-Leu-Arg-amide; RGDS, arginyl-glycyl-L-aspartyl-serine; FMGB·HCl, fluorescein mono-*p*-guanidinobenzoate·hydrochloride; AMC, 7-amino-4-methylcoumarin; Boc-EAR-AMC, Boc-Glu(OBzl)-Ala-Arg-AMC; S-2366, Pyro-Glu-Pro-Arg-*p*-nitroanilide·HCl; HEPES-Tyrodé's buffer, 0.1% bovine serum albumin, 126 mM NaCl, 2.7 mM KCl, 1 mM $\text{MgCl}_2 \cdot 6\text{H}_2\text{O}$, 0.4 mM $\text{NaH}_2\text{PO}_4 \cdot \text{H}_2\text{O}$, 5.6 mM dextrose, 15 mM HEPES, pH 7.4 at 37 °C; PIX1, platelet inhibitor of factor XIa.

² Kunitz relates to the family of proteins having structural homology with aprotinin; an inhibitor originally discovered by Kunitz. The Kunitz family is commonly lumped with the soybean trypsin inhibitor family—the index protein of which also was discovered by Kunitz—and referred to as Kunitz protease inhibitors; however, this term is purely historical and does not reflect structural similarity. Hence, Kunitz is the preferred term (Salvesen & Pizzo, 1994).

it has been suggested that PN-2 may be an important regulator of the procoagulant response to vascular damage (Van Nostrand et al., 1992). However, the ability of PN-2 to regulate hemostasis depends upon the time scale over which it acts. We have conducted detailed kinetic analyses to determine the mechanism and rate constants governing the inhibition of FXIa by PN-2. We have also directly studied the fate of FXIa after platelet stimulation and the release of α -granule contents from activated platelets. Since FXIa circulates in plasma complexed with high molecular weight kininogen (HK), a nonenzymatic cofactor central to the contact phase of blood coagulation (Thompson et al., 1977), we examined the effect of HK on the inhibition of FXIa by PN-2 both in the absence and presence of human platelets.

EXPERIMENTAL PROCEDURES

Materials. PN-2 was purified from fibroblast culture media by sequential heparin affinity chromatography and immunoaffinity chromatography as described previously (Van Nostrand & Cunningham, 1987; Van Nostrand et al., 1990b). The protein was dialyzed overnight against 100 vol of HBS and aliquots of the dialyzed protein were stored at -70°C . Human FXIa was purchased from Haematologic Technologies, Inc. (Essex Junction, VT). Human HK was obtained from Enzyme Research Laboratories, Inc. (South Bend, IN). The thrombin receptor peptide, SFLLRN-amide was synthesized as described previously (Scandura et al., 1996). Bovine trypsin, RGDS, FMGB·HCl, and fluorescein were purchased from Sigma Chemical Co. (St. Louis, MO). The fluorogenic substrate, Boc-EAR-AMC, was obtained from Peptide International, Inc. (Louisville, KY), and the chromogenic substrate, S-2366, was purchased from Chromogenix (Mölnådal, Sweden). All other materials were analytical grade or the highest grade commercially available.

Active-Site Titration of Enzymes. The sensitive active-site titrant FMGB·HCl was used to determine the concentration of both bovine trypsin and FXIa essentially as described (Melhado et al., 1982; Bock et al., 1989). Though not previously reported as such, FMGB·HCl is an extremely useful titrant of FXIa with a very rapid acylation rate and an extremely slow deacylation rate (data not shown). Active-site measurements were made in HEPES-Tyrodé's buffer at room temperature. The release of fluorescein from FMGB·HCl (10 μM) was monitored in a Bowman Series 2 spectrofluorimeter (SLM Aminco, Urbana, IL) both before and after the addition of enzyme. The excitation and emission wavelengths used were 500 and 520 nm, respectively, and 4 nm slit widths were used on both sides. After correcting for the spontaneous hydrolysis of FMGB·HCl, the burst height measured after the addition of trypsin or FXIa was converted to molar units with the use of a standard curve made with known concentrations of fluorescein. Stock solutions of fluorescein and FMGB·HCl were made in dry dimethyl sulfoxide, and their concentrations were measured in 0.1 N NaOH at 490 nm using the molar extinction coefficient of fluorescein ($\epsilon = 89\,320\text{ M}^{-1}\text{ cm}^{-1}$) (Heller et al., 1974).

The burst amplitude is an accurate measure of the total enzyme concentration only when the titrant's concentration is well above the enzyme's K_m . The K_m of trypsin for FMGB·HCl is 5.6 pM (Heller et al., 1974), and, as expected,

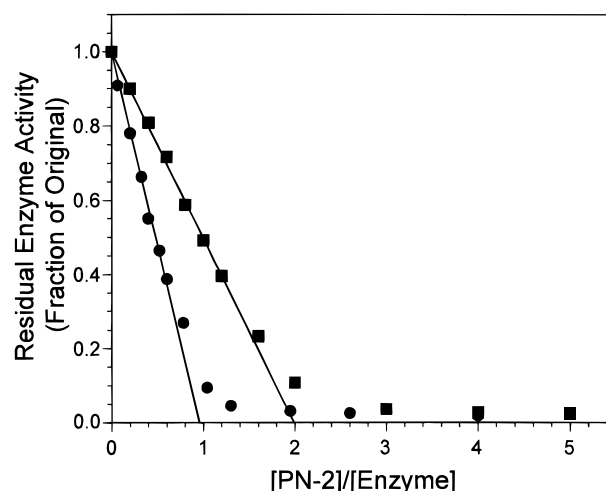


FIGURE 1: Titration of PN-2 with FXIa (■) and Trypsin (●). Active-site titrated trypsin (10 nM) and FXIa (5 nM) were incubated with varying concentrations of PN-2 (0.5–20 nM) for 1 h, at 37°C . After this incubation, the residual activity of the enzymes was determined by measuring the velocity of S-2366 hydrolysis (0.45 mM) at 405 nm. In this experiment, PN-2 interacted with 0.96 active-sites per trypsin molecule and 2.0 active-sites per FXIa molecule.

the burst amplitude was independent of the FMGB·HCl concentration in the range (5–50 μM) used to titrate trypsin. We reasoned that the K_m of FXIa for FMGB·HCl must also be much lower than 5 μM , since we found that the burst amplitude was similarly independent of the FMGB·HCl concentration when FXIa was titrated over this same range (5–50 μM FMGB·HCl) (data not shown).

We found that the active-site measurements of trypsin and FXIa agreed well with the protein concentrations calculated from the absorbance at 280 nm and published extinction coefficients (Chase & Shaw, 1969; Kurachi & Davie, 1977) (the $\epsilon_{280}^{0.1\%}$ values were 1.54 and 1.34 for trypsin and FXIa, respectively). There were 0.8–0.9 active-sites per trypsin molecule and 1.8–2.0 active-sites per FXIa molecule. This measurement is consistent with the dimeric nature of FXIa and suggests that both active-sites can operate independently since both can bind FMGB·HCl simultaneously.

Measurement of PN-2 Reactive Sites. The concentration of PN-2 reactive sites was measured by titrating active-site titrated trypsin with PN-2. A 1:1 (inhibitor:enzyme) stoichiometry was assumed. To wells of a siliconized microtiter plate were added trypsin (10 nM) and PN-2 (0–50 nM) in a total volume of 135 μL HEPES-Tyrodé's buffer. The mixture was allowed to reach equilibrium during a 60 min incubation at ambient temperature. After this incubation, the microtiter plate was warmed to 37°C , 15 μL of the chromogenic substrate, S-2366 (0.45 mM), was added to each well, and the residual enzyme activity was measured as the initial rate of change in the absorbance at 405 nm in a ThermoMax kinetic microplate reader (Molecular Devices, Palo Alto, CA). Once the concentration of PN-2 reactive sites was determined in this way, active-site titrated FXIa (5 nM dimer) was titrated with the PN-2 to determine the stoichiometry of inhibition (see Figure 1). As expected (Smith et al., 1990), PN-2 was found to inhibit FXIa with a stoichiometry of 2:1 (inhibitor:enzyme) reflecting the dimeric nature of FXIa.

Progress Curve Measurements of the Rate of FXIa Inhibition by PN-2. Release of the highly fluorescent

product, AMC, from the peptidyl substrate, Boc-EAR-AMC, by FXIa was monitored in a Bowman Series 2 spectrofluorimeter. The fluorimeter slit widths were set at 4 nm and the excitation and emission wavelengths were 375 and 445 nm, respectively. FXIa (5 or 10 pM) was added to a fluorimeter cuvette containing 2 mL of HEPES-Tyrodé's buffer and 10–25 μ M Boc-EAR-AMC. Hydrolysis of the substrate was recorded for 10 min, and then a small volume (less than 1% of the total volume) of PN-2 (0–10 nM) was added. The progress curves were monitored for over 1 h (at 5–10 s intervals) at 37 °C with continuous, gentle stirring. In the absence of inhibitor, the release of product was linear during the entire measurement period indicating that the FXIa was stable at the low concentrations used.

Progress curves were also used to monitor the dissociation of pre-formed FXIa/PN-2 complexes. In these “dissociation experiments”, equal volumes of FXIa (0.5 or 1 nM) and PN-2 (5–400 nM) were incubated at 37 °C for at least 1 h to allow the reactants to achieve equilibrium. After this initial incubation, the mixture, including pre-formed FXIa/PN-2 complexes, was diluted 100–250-fold into a 2 mL fluorescence cuvette containing Boc-EAR-AMC (25 μ M) in HEPES-Tyrodé's buffer. An increasing rate of AMC release from Boc-EAR-AMC, reflecting the slow dissociation of FXIa/PN-2 complexes, was monitored until a new equilibrium was achieved and the progress curves became linear.

Kinetic Mechanism of FXIa Inhibition by PN-2. Two general mechanisms of competitive inhibition have been described for slow, tight-binding inhibitors (Cha, 1975; Morrison, 1982; Tian & Tsou, 1982; Morrison & Walsh, 1987). In Mechanism A, the equilibrium established between free enzymes, free inhibitors and enzyme–inhibitor complexes is approached slowly and directly. Mechanism B differs in that there is an initial, rapid association between free enzymes and inhibitors which slowly tightens to form a more stable enzyme–inhibitor complex.

Equation 1 is a general equation for progress curves that result from Mechanism A and Mechanism B when pseudo-first-order conditions pertain (Cha, 1975). This equation may be used in the analysis of progress curve data if the concentration of inhibitor remains approximately constant and no significant consumption of substrate occurs during the course of the experiment.

$$P = V_s t + (V_o - V_s) (1 - e^{-k_{obs}t})/k_{obs} \quad (1)$$

In eq 1, V_o is the velocity of product formation at the start of the reaction between the enzyme and inhibitor, V_s is the velocity after a new steady-state has been established, k_{obs} is the observed first-order rate constant which characterizes the transition from the initial velocity to the steady-state velocity, and P is the concentration of product formed at any time, t . Mechanism A and Mechanism B can be distinguished by the manner in which the inhibitor concentration affects V_o and k_{obs} (see eq 2). If the progress curve is the result of Mechanism A, then k_{obs} increases in direct proportion (i.e., linearly) to the inhibitor concentration whereas V_o is independent of the inhibitor concentration (see eq 2 and Figure 3). If, however, Mechanism B pertains, then both k_{obs} and V_o are hyperbolic functions of the inhibitor concentration.

In eq 2, k_{cat} and K_m are the Michaelis–Menten parameters for the reaction between enzyme and substrate. S_o is the

initial substrate concentration and E_T and I_T are the total concentration of enzyme and inhibitor species, respectively. In eq 2, Mechanism A, k_{on} and k_{off} are the second- and first-order kinetic constants with which enzyme–inhibitor complexes form and dissociate, respectively. For Mechanism B (eq 2B), k_{on} and k_{off} are both first-order kinetic constants describing the rates of transition between the initial loose enzyme–inhibitor complex, which has an equilibrium constant K_i , and the tighter complex.

Mechanism A

$$V_o = \frac{k_{cat}E_T S_o}{K_m + S_o}, \quad k_{obs} = k_{off} + \frac{k_{on}I_T}{1 + S_o/K_m} \quad (2A)$$

Mechanism B

$$V_o = \frac{k_{cat}E_T S_o}{K_m(1 + I_T/K_i) + S_o}, \quad k_{obs} = k_{off} + \frac{k_{on}I_T}{K_i(1 + S_o/K_m) + I_T} \quad (2B)$$

Progress Curve Analysis. Progress curves were measured after either the addition of inhibitor to a mixture of enzyme and substrate (“association experiments”) or after the dilution of pre-incubated enzyme–inhibitor mixtures into substrate containing solutions (“dissociation experiments”). Sets of five to ten such progress curves were generated by varying the concentration of inhibitor while holding constant the concentrations of enzyme and substrate.

Progress curves were analyzed with eq 1 since both of the assumptions inherent to this equation were valid: the inhibitor concentration changed by only 0.5%–2% and less than 0.1% of the substrate was consumed during the time course of the experiment. Initially, we analyzed data from “association experiments” to determine the mechanism of FXIa inhibition by PN-2. For this reason, eq 1 was fit to each progress curve individually using the program Kaleidagraph v3.0.5 (Abelbeck Software) which utilizes the Levenberg–Marquardt algorithm (Marquardt, 1963) for nonlinear least-squares regression. The parameters, V_o , V_s , and k_{obs} , obtained for each curve were then analyzed within the contexts of Mechanism A and Mechanism B using eq 2A,B. Once we had established that the inhibition of FXIa by PN-2 was well described by Mechanism A (see Results), subsequent analysis was carried out within the context of this mechanism. All curve fits and simulations were run on a PowerMac 8100 personal computer (Apple Computer, Inc., Cupertino, CA).

The data points collected during the transition from V_o to V_s contain most of the information useful in obtaining estimates of k_{on} and k_{off} . In “association experiments”, this transition is most pronounced at high inhibitor concentrations where k_{obs} is strongly influenced by k_{on} . The opposite is true for “dissociation experiments” which contain more kinetic information at low inhibitor concentrations where k_{obs} is close to k_{off} . Hence, the experimental conditions are such that “association experiments” are more useful for obtaining estimates of k_{on} and “dissociation experiments” are better for estimating k_{off} , particularly, when k_{off} is small. “Dissociation experiments” were also analyzed with eq 1; however, the different initial conditions require a different

equation for V_o (see eq 3A,B). Since, in a “dissociation experiment”, the initial incubation between enzyme and inhibitor occurs in a more concentrated solution the equation for V_o includes the term, D , to reflect the dilution factor of the final mixture.

Association Experiments

$$V_o = \frac{k_{\text{cat}}E_T S_o}{K_m + S_o} \quad (3A)$$

Dissociation Experiments

$$V_o = \frac{k_{\text{cat}}E_T S_o}{K_m(1 + DI_T k_{\text{on}}/k_{\text{off}}) + S_o} \quad (3B)$$

After the mechanism of inhibition had been established, estimates of the rate constants (i.e., k_{on} and k_{off}) were obtained by fitting sets of five to ten progress curves, measured at different PN-2 concentrations, simultaneously to eq 1; the appropriate substitutions from eqs 2 and 3 were included. A Visual Basic module was written for Microsoft Excel v5 (Microsoft Corp., Redmond, WA) to carry out all calculations and curve fits. Parameters other than the rate constants were fixed during the curve-fitting procedure. E_T , I_T , S_o , and D were set to their independently measured values, and the terms containing the Michaelis–Menten kinetic parameters, for FXIa-catalyzed hydrolysis of Boc-EAR-AMC, were treated as constants.

We were not able to confirm the published K_m of Boc-EAR-AMC for FXIa (i.e., 370 μM) (Kawabata et al., 1988), nor were we able to define a reliable estimate of the K_m . We found that the K_m exceeded the solubility of Boc-EAR-AMC (the solubility in HBS and HEPES-Tyrodé's was $\sim 600 \mu\text{M}$) in all of the aqueous buffers tested. We estimated the K_m to be well above the solubility of Boc-EAR-AMC since the initial velocity increased linearly with the substrate concentration until the solubility limit was reached and the velocity became constant (data not shown). In our progress curve measurements, we used a substrate concentration (10–25 μM) that was insignificant when compared to the minimum possible K_m (600 μM). Under such circumstances, the concentration of the Michaelis complex ($E \cdot S$) is negligible when compared to the total concentration of enzyme (i.e., $E \cdot S \ll E_T$) and the apparent forward rate constant, $k_{\text{on,app}}$, will be very close to the true forward rate constant, k_{on} (see eq 4): at most, there could be a 4% difference between k_{on} and $k_{\text{on,app}}$.

Measurements of the Equilibrium Inhibition Constant, K_i . Equation 4 is used to calculate an apparent K_i , $K_{i,\text{app}}$, from the kinetic parameters obtained from the analysis of progress curves. Since the conditions under which the progress curves are measured are such that the $S_o \ll K_m$, $K_{i,\text{app}}$ is approximately equal to the true K_i .

$$K_{i,\text{app}} = \frac{k_{\text{off}}}{k_{\text{on,app}}} = \frac{k_{\text{off}}}{k_{\text{on}}/(1 + S_o/K_m)} = K_i(1 + S_o/K_m) \quad (4)$$

K_i can also be directly measured by allowing FXIa and PN-2 to come to equilibrium. Equilibrium measurements were conducted as follows: (1) a fixed concentration of FXIa (0.1 or 0.25 nM), HK (0–500 nM), and Zn^{2+} (0 or 25 μM)

and one of eight different concentrations of PN-2 (0–10 nM) were incubated for 1–2 h at 37 °C in a total volume of 300 μL of HEPES-Tyrodé's buffer; (2) the FXIa substrate, S-2366 (0.6 mM), was then added to the mixture and the initial reaction velocity was monitored at 405 nm in a Hewlett-Packard 8452A diode array spectrophotometer (Wilmington, DE) for 10 min. Less than 5% of the substrate was consumed during the 10 min measurement, and the reaction was entirely linear. The velocities observed at each PN-2 concentration were normalized to the velocity measured in the absence of PN-2; thus, the fraction of FXIa activity was determined. This fraction of residual FXIa activity was plotted against the concentration of PN-2 (e.g., Figure 5) and the apparent inhibition constant, $K_{i,\text{app}}$, was obtained from a least-squares fit of these data to eq 5.

$$\frac{V_s}{V_o} = 1 - \{[(E_T + I_T + K_{i,\text{app}}) - \sqrt{(E_T + I_T + K_{i,\text{app}})^2 - 4I_T E_T}]/2E_T\} \quad (5)$$

Although we measured the K_m for S-2366 to be $350 \pm 20 \mu\text{M}$ (data not shown), we found the $K_{i,\text{app}}$ to be independent of the S-2366 concentration (0.15–0.9 mM) used. Since the rate with which the FXIa/PN-2 complexes dissociate is very slow, the concentration of free FXIa does not change to any significant degree during the 10 min measurement period. In essence, we measure the concentration of free enzyme after the pre-incubation had reached equilibrium. Hence, $K_{i,\text{app}}$ was equal to the true K_i .

Release of FXIa Inhibitors from Activated Platelets. Seven volumes of fresh human blood was drawn from a healthy donor into 1 vol of acid-citrate–dextrose anticoagulant (71 mM citric acid, 85 mM trisodium citrate, 111 mM dextrose). Platelets were prepared by modified sequential albumin density gradient isolation followed by gel filtration on a Sepharose 2B column equilibrated with HEPES-Tyrodé's buffer (Walsh et al., 1977). The isolated platelets were counted electronically using a model ZM Coulter Counter (Coulter Electronics, Hialeah, FL). The platelet concentration was adjusted to 0.5 or $1 \times 10^8/\text{mL}$ before placing the platelet suspension into a fluorimeter cuvette maintained at 37 °C with continuous gentle stirring. The tetrapeptide RGDS (0.1 mM) was added to prevent platelet aggregation. Boc-EAR-AMC (25 μM) was then added followed by the addition of FXIa (25 or 50 pM). The hydrolysis of Boc-EAR-AMC was measured for 10 min before the addition of the thrombin receptor peptide, SFLLRN-amide (12.5 μM), and up to 1 h afterward. The manner with which HK and Zn^{2+} affected the inhibition of FXIa after platelet activation was compared to the effect that these compounds have on the inhibition of FXIa by PN-2.

RESULTS

Kinetic Mechanism of FXIa Inhibition by PN-2. The prolonged transient phase observed for the inhibition of FXIa by PN-2 (Figure 2) is characteristic for a slow-binding inhibitor (Morrison & Walsh, 1987) and is typical of members of the Kunin class of protease inhibitors. This qualitative result agrees well with the observations of other authors (Smith et al., 1990; Van Nostrand et al., 1990a). However, it has not been reported whether PN-2 inhibits

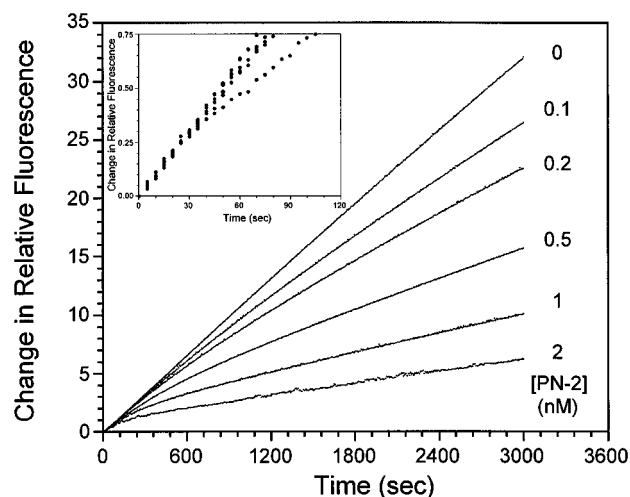


FIGURE 2: Progress curves of FXIa amidolytic activity after the addition of PN-2. The reaction was started by the addition of concentrated PN-2 to 2 mL of HEPES-Tyrod's buffer containing 25 μ M Boc-EAR-AMC and 10 pM FXIa. The final concentrations of PN-2 (0, 0.1, 0.2, 0.5, 1, and 2 nM) are shown on the right-hand side of the graph. All reactions were conducted at 37 $^{\circ}$ C and were stirred continuously. (Inset) Progress curves just after the addition of PN-2.

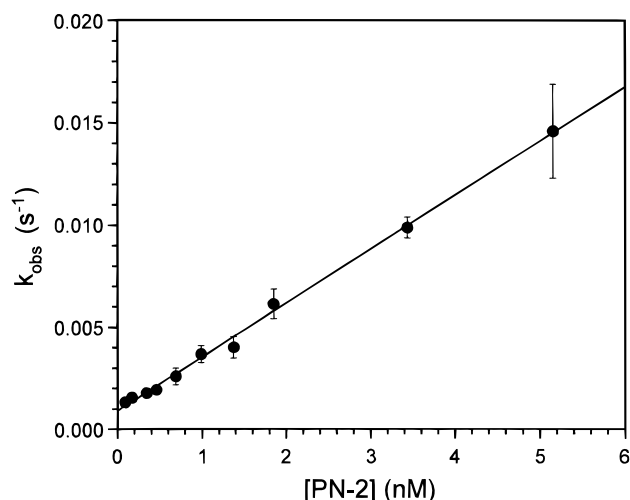


FIGURE 3: Dependence of k_{obs} upon the concentration of PN-2. The k_{obs} values were obtained by fitting progress curve data such as that in Figure 2 to eq 1. Each value represents the average k_{obs} obtained from nine independent progress curves. The error bars reflect the standard error in the mean for each value. The solid line represents a nonlinear least-squares fit of these data to eq 2A. The best fit parameters to this data are $k_{\text{on}} = 2.6 \times 10^6 \text{ M}^{-1} \text{ s}^{-1}$ and $k_{\text{off}} = 9.1 \times 10^{-4} \text{ s}^{-1}$.

FXIa by Mechanism B, as Kunin inhibitors commonly do, or if Mechanism A adequately describes this inhibition.

To distinguish these two basic mechanisms, progress curve data were fitted to eq 1 and estimates of V_o , V_s , and k_{obs} were obtained. As the PN-2 concentration increases, the initial rate of product formation (V_o) does not vary (Figure 2, inset) and k_{obs} increases linearly (Figure 3) with the PN-2 concentration (up to 10 nM). Thus, under our assay conditions, the inhibition of FXIa by PN-2 conforms to Mechanism A.

Analysis of Progress Curves. Equation 2 can be used to calculate k_{on} and k_{off} from the slope and intercept of the line fit to the data in Figure 3. These values ($k_{\text{on}} = 2.6 \times 10^6 \text{ M}^{-1} \text{ s}^{-1}$ and $k_{\text{off}} = 9.1 \times 10^{-4} \text{ s}^{-1}$) are in close agreement with the average values obtained by simultaneously fitting

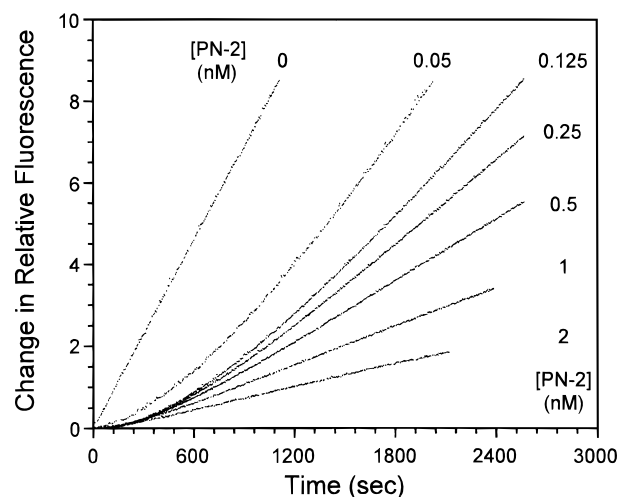


FIGURE 4: Progress curves of FXIa amidolytic activity after the dilution of pre-formed FXIa/PN-2 complexes. FXIa (0.5 nM) was incubated with PN-2 (5–200 nM) at 37 $^{\circ}$ C for 1 h. The mixture was then diluted 100-fold into HEPES-Tyrod's buffer containing Boc-EAR-AMC (25 μ M). The hydrolysis of the Boc-EAR-AMC was measured continuously for up to 45 min, at which point the reaction rate became linear.

families³ of curves from “association experiments” (e.g., see Figure 2) or “dissociation experiments” (e.g., see Figure 4) to eq 1 (with appropriate substitutions from eq 2 and eq 3). Fitting 23 such families of curves to eq 1 yields an average association rate constant (k_{on}) of $2.1 (\pm 0.2) \times 10^6 \text{ M}^{-1} \text{ s}^{-1}$ and an average dissociation rate constant (k_{off}) of $8.5 (\pm 0.8) \times 10^{-4} \text{ s}^{-1}$, respectively ($n = 23$). The inhibition constant (K_i) calculated from these parameter values is $400 \pm 50 \text{ pM}$.

Effect of HK and Zn^{2+} Ions on the Activity of PN-2. The inhibition constant (K_i) for FXIa was also determined at equilibrium by measuring the initial velocity of S-2366 cleavage by FXIa after pre-incubation of the FXIa with varying concentrations of PN-2 (see Experimental Procedures). The residual FXIa activity was plotted as shown in Figure 5, and data were fit to eq 5 to obtain an estimate of the K_i . The average K_i value was $370 \pm 24 \text{ pM}$ ($n = 25$) in the absence of HK and ZnCl_2 and is in good agreement with the value calculated from the kinetic parameters as well as with the results of other authors (Smith et al., 1990; Van Nostrand et al., 1990a). We found that HK alone protects FXIa from inactivation in a dose-dependent manner (Figure 6). The EC_{50} of HK is $\sim 60 \text{ nM}$ and, at the physiological concentration of HK ($\sim 500 \text{ nM}$), the K_i for PN-2 is increased to $\sim 980 \text{ pM}$. Zn^{2+} enhances the ability of PN-2 to inhibit FXIa and, the optimal concentration of Zn^{2+} (25 μM)—a value close to the physiological concentration of Zn^{2+} ions—induces a 3-fold decrease in the K_i to $\sim 140 \text{ pM}$. Below a concentration of 5 μM , Zn^{2+} ions do not affect the inhibition of FXIa by PN-2. Curiously, high Zn^{2+} concentrations ($\geq 50 \mu\text{M}$) inhibit the amidolytic activity of FXIa (data not shown). The protective effect of HK on FXIa was abolished when 25 μM Zn^{2+} was included with HK in the incubations (Figure 6).

Secretion of FXIa Inhibitors from Activated Platelets. When isolated platelets were activated by SFLLRN-amide,

³ We use the terms “sets” and “families” of progress curves to indicate the five to ten progress curves conducted on a single day at five to ten different PN-2 concentrations and at fixed FXIa and substrate concentrations.

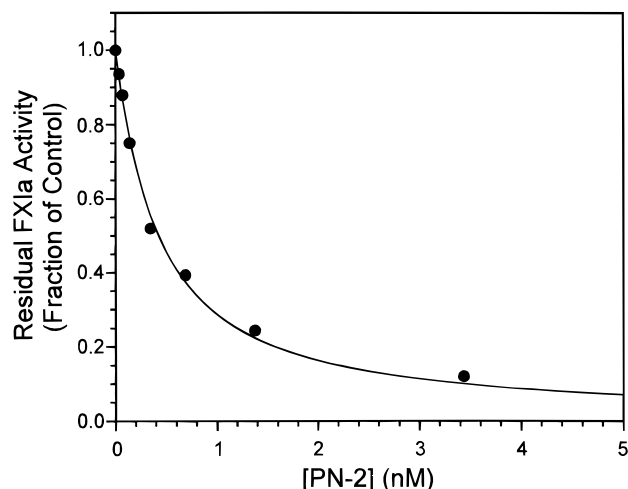


FIGURE 5: Measurement of the inhibition constant (K_i) at equilibrium. Shown is a representative experiment wherein FXIa and PN-2 were pre-incubated for 1 h and then the residual FXIa amidolytic activity was measured. The data (●) were normalized to the FXIa activity measured in the absence of PN-2. The K_i determined from the best fit of these data to eq 5 was found to be 370 pM.

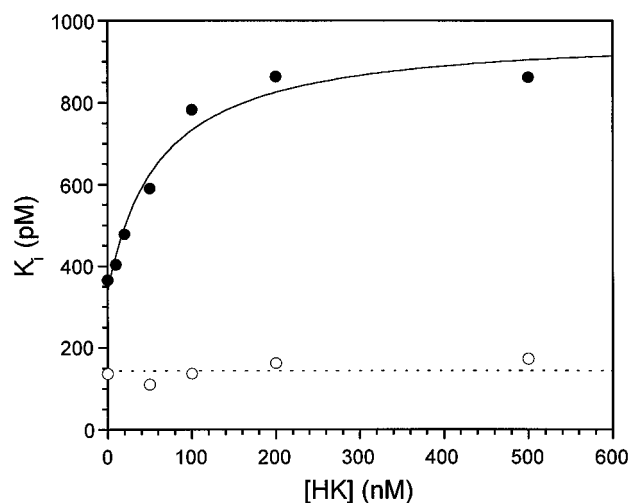


FIGURE 6: Effect of HK and Zn^{2+} ions on FXIa inhibition by PN-2. K_i was determined in the presence of HK alone (●), and HK plus $ZnCl_2$ (25 μM) (○) essentially as described in Figure 5. Each point represents the average of three measurements. In the absence of Zn^{2+} , the effect of HK on the K_i of PN-2 had an EC_{50} of 61 nM and saturated at a value of 980 pM (—). In the presence of Zn^{2+} , HK had no discernible effect on the K_i which remained constant at 140 pM (---).

significant inhibition of FXIa was observed (Figure 7). The amount of inhibition was dependent upon the concentration of platelets used. If all of this inhibitory activity were the result of PN-2 release, the total amount of PN-2 released would need be 3–5 nM per 3×10^8 platelets. Hence, the concentration of PN-2 in whole blood within the locus of a platelet thrombus could easily exceed the K_i for FXIa inhibition by more than 10-fold.

This surprising result prompted us to investigate the ability of HK and Zn^{2+} to affect the inhibition of FXIa—ostensibly by PN-2—observed after platelets are activated by SFLLRN-amide. In the absence of HK, Zn^{2+} ions (25 μM) significantly potentiated the inhibition of FXIa after platelet activation whereas HK, in the absence of Zn^{2+} , decreased the extent of FXIa inhibition (Figure 8). However, in contrast to the results obtained with purified PN-2 alone

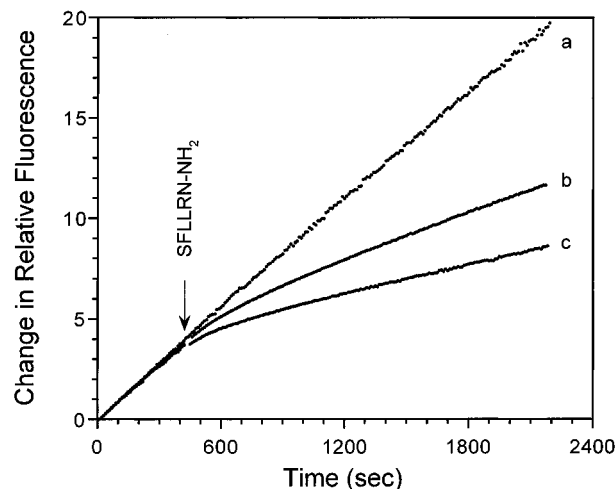


FIGURE 7: Progress curves of FXIa amidolytic activity before and after the activation of human platelets. FXIa (25 pM) was added to human platelets at (a, b) $0.5 \times 10^8/mL$ or (c) $1 \times 10^8/mL$ suspended in HEPES-Tyrod's buffer containing the fluorescent substrate, Boc-EAR-AMC (25 μM). The mixture was stirred continuously and maintained at 37 °C. The cleavage of Boc-EAR-AMC was monitored for 7 min before and up to 1 h after the addition of (a) buffer or (b, c) SFLLRN-amide (25 μM).

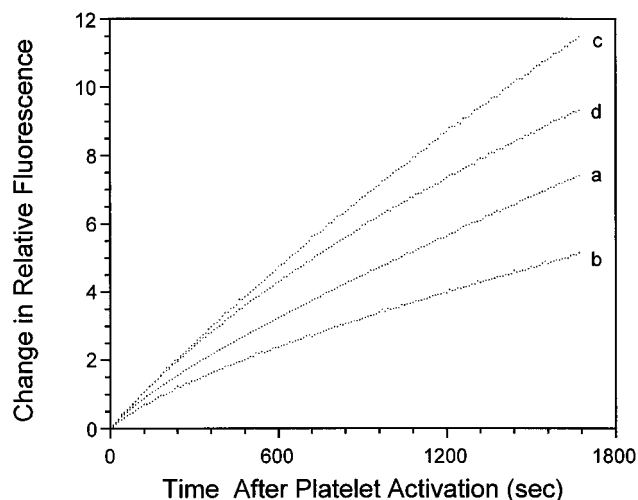


FIGURE 8: Effect of HK and Zn^{2+} on the inactivation of FXIa after platelet activation. The inhibition of FXIa amidolytic activity subsequent to the activation of human platelets ($5 \times 10^7/mL$) by SFLLRN-amide was monitored (a) in the absence of both HK and $ZnCl_2$, (b) in the presence of $ZnCl_2$ (25 μM) alone, (c) in the presence of HK (500 nM) alone, and (d) in the presence of both HK (500 nM) and $ZnCl_2$ (25 μM).

(Figure 6), HK abrogated the effect of Zn^{2+} when both were included in the reaction mixture (Figure 8).

DISCUSSION

We have described experiments wherein the hydrolysis of a sensitive fluorogenic substrate (Boc-EAR-AMC) by FXIa has been monitored in the presence and absence of PN-2, HK, Zn^{2+} , and human platelets. We have also measured the effects of HK and Zn^{2+} on the equilibrium constant, K_i , with which PN-2 inhibits FXIa. From these data, we have ascertained the following: (1) the mechanism and kinetic rate constants for the inhibition of FXIa by PN-2; (2) that HK, the plasma cohort of FXIa, protects FXIa from inhibition by PN-2; (3) that Zn^{2+} accentuates the ability of PN-2 to inhibit FXIa; (4) that, coincident with the activation of human platelets, there is a slow inhibition of

FXIa activity; that HK slows and limits this inhibition and that Zn^{2+} quickens and enhances this inhibition; (5) that, in solution, Zn^{2+} completely abrogates the protection from PN-2 that HK affords to FXIa; and (6) that HK suppresses the FXIa inhibition observed coincident with platelet activation whether Zn^{2+} is present or not.

We examined the inactivation of FXIa by PN-2 by analyzing progress curves and have found this to be a powerful technique. The kinetics of slow inhibitors are well-suited to progress curve analysis using common and relatively inexpensive laboratory equipment since these reactions occur on a time scale that obviates the need for stopped- or quenched-flow equipment. We used a highly sensitive fluorogenic substrate, Boc-EAR-AMC,⁴ to permit the use of enzyme concentrations low enough to ensure that neither significant substrate depletion nor product inhibition occurred even when the reactions were monitored for extended periods of time: The reaction was entirely linear in the absence of inhibitor and, when inhibitor was present, the shape of the progress curve was strongly influenced by the inhibition step. Continuously monitoring the reaction instead of measuring discrete sub-samples (e.g., initial rates after fixed intervals) had several tangible benefits: (1) information about the entire time course of the reaction was obtained, (2) the consumption of reagents was reduced, and (3) the experiments were simple to perform.

We generated progress curve data using pseudo first-order conditions (see Figures 2 and 4). Equation 1 was used to analyze this data and enabled us to differentiate Mechanism A from Mechanism B: two common mechanisms of tight-binding inhibitors. We found that at the inhibitor concentrations used (≤ 5 nM), PN-2 inhibits FXIa by the direct formation (i.e., via Mechanism A) of enzyme-inhibitor complexes and with a 1:2 stoichiometry. Inherent to our analysis of FXIa inhibition by PN-2 is the assumption that the two active-sites of FXIa can be treated as independent enzymes, with catalytic activities that are independent of each other, and which each interact with PN-2 in an unconstrained and equivalent manner. The validity of this assumption is supported by the absence of cooperativity apparent in both kinetic and equilibrium measurements (see Figures 3 and 5, respectively).

We found that our estimates of k_{off} and k_{on} were independent of the method by which they were abstracted from the data. The values obtained by plotting the trends in the k_{obs} values obtained after fitting individual progress curves to eq 1 (as shown in Figure 3) were essentially identical to the values obtained by simultaneously fitting families of curves from "association" or "dissociation" experiments to eq 1 (with substitutions from eqs 2 and 3). We also found that the overall equilibrium inhibition constant, K_i , was the same whether it was calculated from the ratio of the forward and reverse rate constants or measured directly (e.g., see Figure 5).

We investigated the effects of HK and Zn^{2+} ions on the inhibition of FXIa by PN-2. We found that HK protects FXIa from inhibition by PN-2 in a dose-dependent and saturable manner (see Figure 6). HK maximally increases the K_i for PN-2 to 980 pM and the EC_{50} (60 nM) with which HK does this is very close to the K_d with which HK binds

FXIa (Scott et al., 1982; Warn-Cramer & Bajaj, 1985), suggesting that HK is an allosteric modulator of FXIa inhibition by PN-2. Whether HK also protects FXIa from inhibition by plasma protease inhibitors of the Serpin family is unclear: HK has been shown to inhibit (Scott et al., 1982), enhance (Olson et al., 1992), and have no effect (Meijers et al., 1988) upon the inactivation of FXIa. In contrast to the protective effect of HK, Zn^{2+} ions accentuate the ability of PN-2 to inhibit FXIa (Van Nostrand, 1995) (see Figure 6). At a plasma Zn^{2+} concentration (~ 25 μM), we found the K_i for FXIa inhibition by PN-2 to be 140 pM. Since HK and Zn^{2+} ions exert opposite effects on this inhibition, it is remarkable that when both HK and Zn^{2+} are present, only the effect of Zn^{2+} is seen: the protective effect of HK is completely abrogated (Figure 6). Both HK and PN-2 are known to possess Zn^{2+} binding sites (DeLa Cadena & Colman, 1992; Bush et al., 1993) and it is tempting to postulate the existence of an HK domain which disrupts the association of FXIa and PN-2 in the absence of Zn^{2+} but attains a non-interfering conformation when Zn^{2+} ions are present; however, we have no direct evidence of such a zinc-dependent domain.

HK and Zn^{2+} have both been shown to affect the behavior of FXI(a) in purified and partially purified systems. In plasma, each subunit of FXI is associated with a single HK molecule (Thompson et al., 1977; Warn-Cramer & Bajaj, 1985) and HK is known to be a critical cofactor in the contact pathway activation of FXI [see DeLa Cadena et al. (1994) for review]. Whereas HK has been reported to inhibit the surface-independent activation of FXI by thrombin (Scott & Colman, 1992; von dem Borne et al., 1994), Zn^{2+} ions can enhance it (Gailani & Broze, 1993). HK and Zn^{2+} ions strongly influence the binding of FXI to activated platelets (Greengard et al., 1986) and are required for FXIa to bind to activated platelets (Sinha et al., 1984). Zinc ions are also known to affect the binding of HK to the surface of activated platelets (Greengard & Griffin, 1984).

Platelets are known to secrete several inhibitors upon activation. Though most are secreted in extremely low concentrations [see Schmaier (1985) for review], two have been reported to be secreted in kinetically relevant quantities: PN-2 (Kirschner et al., 1986; Van Nostrand et al., 1990a; Komiyama et al., 1992) and PIXI (Cronlund & Walsh, 1992). We investigated the effect on FXIa activity of platelet activation. We found that the FXIa activity is stable in the presence of unstimulated platelets (see Figure 7) but, subsequent to platelet activation with SFLLRN-amide, there is a time-dependent diminution of FXIa activity. The rate and extent of this inhibition increases as the platelet concentration is increased. The slow disappearance of FXIa activity after platelet activation may represent the inhibition of FXIa by a slow inhibitor or it may simply reflect the time-dependent release of a rapid FXIa inhibitor from platelets. Studies from this laboratory have described a partially characterized, small, mixed-type non-competitive inhibitor of FXIa, PIXI (Cronlund & Walsh, 1992). Though it was initially estimated that PIXI contributed 18%–54% of the FXIa inhibitory activity found in platelet releasates, we have since found⁵ that the true contribution of PIXI is probably less than 10%. This estimate is more in line with the observations of Smith and Broze (1992) who found that PN-2

⁴ Boc-EAR-AMC is approximately 1000-fold more sensitive than the chromogenic substrate most commonly used for FXIa, S-2366.

⁵ Chang-Jun Hu and Peter N. Walsh, unpublished observations.

accounts for >95% of the FXIa inhibitory activity found in platelet releasates. We have also found that the inhibitory activity observed concomitant with platelet activation does not appear to be associated with the platelet surface after platelets are activated since $\geq 90\%$ of the inhibitory activity remains in the supernatant after the activated platelet suspensions have been centrifuged at 15000g to remove platelets and platelet membrane fragments [data not shown; see also Smith et al. (1990)]. Workers from this laboratory⁵ have also shown that greater than 90% of the inhibitory activity contained in platelet releasates comigrates with PN-2 on a gel-filtration column. Thus, it seems likely that most of the inhibition we observe after platelet activation is due to the release of PN-2. We were unable to demonstrate this conclusively since two monoclonal antibodies directed against the Kunin domain of PN-2 were unable to prevent the inhibition of FXIa by PN-2 in purified systems (data not shown). We were, however, able to demonstrate that, at a concentration of 7.5 nM, mouse nerve growth factor (7S), which is inhibited by PN-2 with a K_i of 9.1 nM (Van Nostrand et al., 1990b), is able to reduce the inhibition of FXIa by PN-2 by $\sim 50\%$ in purified systems and also reduces to a similar extent the inhibition of FXIa by platelet releasates. These considerations are consistent with the view that the major FXIa inhibitor secreted from human platelets is PN-2.

Quantitative immunoblotting studies have shown that activated platelets contribute 160 ng of PN-2/ 10^8 platelets whereas plasma contains virtually no PN-2 (Van Nostrand et al., 1990a; Komiyama et al., 1992). We estimate from the linear portions of our progress curve measurements that 1–1.5 nM of PN-2 is released per 10^8 platelets, in excellent agreement with other published estimates (Van Nostrand et al., 1990a; Komiyama et al., 1992). Thus, at physiological platelet concentrations (3×10^8 platelets per mL of blood), the concentration of PN-2 may be brought to 3–5 nM; the concentration within a nascent thrombus may be even higher. We have shown that the amount of platelet-secreted inhibitor (PN-2) is sufficient to curtail the lifetime of FXIa activity within the locus of activated platelets.

Consistent with their effects on the inhibition of FXIa by PN-2, HK and Zn^{2+} exert opposite effects on the inactivation of FXIa observed coincident with platelet activation (see Figure 8). HK, at its plasma concentration, limits the extent to which FXIa is inhibited to roughly 10% of that seen in the absence of HK (see Figure 8, line c). Zn^{2+} ions bring about almost twice the inhibition of FXIa after platelet activation (see Figure 8, line b). However, unlike what was seen in the purified system, it is the protective effect of HK that predominates when both HK and Zn^{2+} are present in the presence of activated platelets (see Figure 8, line d). We cautiously suggest that the different behavior observed in the presence of activated platelets may result from the binding of FXIa to the platelet surface in the presence of HK and Zn^{2+} ions (Sinha et al., 1984) and its protection from inactivation when on the platelet surface (Walsh et al., 1987).

The precise physiological role of PN-2 in blood coagulation has not been fully elucidated. In addition to inhibiting FXIa, PN-2 also has been found to inhibit blood coagulation factors IXa and Xa (Schmaier et al., 1993, 1995; Mahdi et al., 1995). However, when the $K_{i,\text{app}}$ for PN-2 inhibition of FIXa ($K_{i,\text{app}} \approx 25$ nM) in the intrinsic pathway FXase complex (i.e., FIXa, FVIIIa, Ca^{2+} , and a surface) (Schmaier

et al., 1995) and for FXa ($K_{i,\text{app}} \approx 19$ nM) in the prothrombinase complex (i.e., FXa, FVa, Ca^{2+} , and a surface) (Mahdi et al., 1995) is compared to that for FXIa ($K_i \approx 0.4$ nM), it is apparent that PN-2 is more significant as an inhibitor of FXIa.

REFERENCES

- Adams, R. D., & Victor, M. (1993) in *Principles of Neurology*, McGraw-Hill, Inc., New York.
- Ahmad, S. S., Rawala-Sheikh, R., & Walsh, P. N. (1989) *J. Biol. Chem.* 264, 3244.
- Bock, P. E., Craig, P. A., Olson, S. T., & Singh, P. (1989) *Arch. Biochem. Biophys.* 273, 375.
- Bush, A. I., Martins, R. N., Rumble, B., Moir, R., Fuller, S., Milward, E., Currie, J., Ames, D., Weidemann, A., Fischer, P., Multhaup, G., Beyreuther, K., & Masters, C. L. (1990) *J. Biol. Chem.* 265, 15977.
- Bush, A. I., Moir, R. D., Multhaup, G., Williamson, T. G., Rumble, B., Small, D. H., Beyreuther, K., & Masters, C. L. (1993) *J. Biol. Chem.* 268, 16109.
- Cha, S. (1975) *Biochem. Pharmacol.* 24, 2177.
- Chase, T., & Shaw, E. (1969) *Biochemistry* 8, 2212.
- Cronlund, A. L., & Walsh, P. N. (1992) *Biochemistry* 31, 1685.
- DeLa Cadena, R. A., & Colman, R. W. (1992) *Protein Sci.* 1, 151.
- DeLa Cadena, R. A., Wachtfogel, Y. T., & Colman, R. W. (1994) in *Hemostasis and Thrombosis: Basic Principles and Clinical Practice* (Colman, R. W., Hirsh, J., Marder, V. J., & Salzman, E. W., Eds.) pp 219–240, J. B. Lippincott Co., Philadelphia, PA.
- Gailani, D., & Broze, G. J. (1993) *Blood Coagulation Fibrinolysis* 4, 15.
- Gardella, J. E., Ghiso, J., Gorgone, G. A., Marratta, D., Kaplan, A. P., Frangione, B., & Gorevic, P. D. (1990) *Biochem. Biophys. Res. Commun.* 173, 1292.
- Gardella, J. E., Gorgone, G. A., Newman, P., Frangione, B., & Gorevic, P. D. (1992) *Neurosci. Lett.* 138, 229.
- Gardella, J. E., Gorgone, G. A., Munoz, P. C., Ghiso, J., Frangione, B., & Gorevic, P. D. (1994) *Lab. Invest.* 67, 303.
- Greengard, J. S., & Griffin, J. H. (1984) *Biochemistry* 23, 6863.
- Greengard, J. S., Heeb, M. J., Ersdal, E., Walsh, P. N., & Griffin, J. H. (1986) *Biochemistry* 25, 3884.
- Heller, C. A., Henry, R. A., McLaughlin, B. A., & Bliss, D. E. (1974) *J. Chem. Eng. Data* 19, 214.
- Kawabata, S., Miura, T., Morita, T., Kato, H., Fujikawa, K., Iwanaga, S., Takada, K., Kimura, T., & Sakakibara, S. (1988) *Eur. J. Biochem.* 172, 17.
- Kirschner, D. A., Abraham, C., & Selkoe, D. J. (1986) *Proc. Natl. Acad. Sci. U.S.A.* 83, 503.
- Kitaguchi, N., Takahashi, Y., Tokushima, Y., Shiojiri, S., & Ito, H. (1988) *Nature* 331, 530.
- Komiyama, Y., Murakami, T., Egawa, H., Okubo, S., Yasunaga, K., & Murata, K. (1992) *Thromb. Res.* 66, 397.
- Kurachi, K., & Davie, E. W. (1977) *Biochemistry* 16, 5831.
- Li, Q. X., Berndt, M. C., Bush, A. I., Rumble, B., Mackenzie, I., Friedhuber, A., Beyreuther, K., & Masters, C. L. (1994) *Blood* 84, 133.
- Mahdi, F., Van Nostrand, W. E., & Schmaier, A. H. (1995) *J. Biol. Chem.* 270, 23468.
- Marquardt, D. W. (1963) *J. Soc. Ind. Appl. Math.* 11, 431.
- Meijers, J. C. M., Vlooswijk, R. A., & Bouma, B. N. (1988) *Biochemistry* 27, 959.
- Melhado, L. L., Peltz, S. W., Leytus, S. P., & Mangel, W. F. (1982) *J. Am. Chem. Soc.* 104, 7299.
- Morrison, J. F. (1982) *Trends Biochem. Sci.* 7, 102.
- Morrison, J. F., & Walsh, C. T. (1987) *Adv. Enzymol.* 61, 201.
- Olson, S. T., Sheffer, R., & Shore, J. D. (1992) *Agents Actions* 38, 241.
- Oltersdorf, T., Fritz, L. C., Schenk, D. B., Lieberburg, I., Johnson-Wood, K. L., Beattie, E. C., Ward, P. J., Blacher, R. W., Dovey, H. F., & Sinha, S. (1989) *Nature* 341, 144.
- Ponte, P., Gonzalez-DeWhit, P., Schilling, J., Miller, J., Hsu, D., Greenberg, B., Davis, K., Wallace, W., Lieberburg, I., Fuller, F., & Cordell, B. (1988) *Nature* 331, 525.

- Salvesen, G., & Pizzo, S. V. (1994) in *Hemostasis and Thrombosis: Basic Principles and Clinical Practice* (Colman, R. W., Hirsh, J., Marder, V. J., & Salzman, E. W., Eds.) pp 251, J. B. Lippincott Co., Philadelphia, PA.
- Scandura, J. M., Ahmad, S. S., & Walsh, P. N. (1996) *Biochemistry* 35, 8890.
- Schmaier, A. H. (1985) *Sem. Hematol.* 22, 187.
- Schmaier, A. H., Dahl, L. D., Rozemuller, A. J. M., Roos, R. A. C., Wagner, S. L., Chung, R., & Van Nostrand, W. E. (1993) *J. Clin. Invest.* 92, 2540.
- Schmaier, A. H., Dahl, L. D., Hasan, A. A. K., Cines, D. B., Bauer, K. A., & Van Nostrand, W. E. (1995) *Biochemistry* 34, 1171.
- Scott, C. F., & Colman, R. W. (1992) *Proc. Natl. Acad. Sci. U.S.A.* 89, 11189.
- Scott, C. F., Schapira, M., James, H. L., Cohen, A. B., & Colman, R. W. (1982) *J. Clin. Invest.* 69, 844.
- Sinha, D., Seaman, F. S., Koshy, A., Knight, L. C., & Walsh, P. N. (1984) *J. Clin. Invest.* 73, 1550.
- Smith, R. P., & Broze, G. J. (1992) *Blood* 80, 2252.
- Smith, R. P., Higuchi, D. A., & Broze, G. J. (1990) *Science* 248, 1126.
- Tanzi, R. E., McClatchey, A. I., Lamperti, E. D., Villa-Komaroff, L., Gusella, J. F., & Neve, R. L. (1988) *Nature* 331, 528.
- Thompson, R. E., Mandle, R., Jr., & Kaplan, A. P. (1977) *J. Clin. Invest.* 60, 1376.
- Tian, W. X., & Tsou, C. L. (1982) *Biochemistry* 21, 1028.
- Van Nostrand, W. E. (1995) *Thromb. Res.* 78, 43.
- Van Nostrand, W. E., & Cunningham, D. D. (1987) *J. Biol. Chem.* 262, 8508.
- Van Nostrand, W. E., Wagner, S. L., Suzuki, M., Choi, B. H., Farrow, J. S., Geddes, J. W., Cotman, C. W., & Cunningham, D. D. (1989) *Nature* 341, 546.
- Van Nostrand, W. E., Schmaier, A. H., Farrow, J. S., & Cunningham, D. D. (1990a) *Science* 248, 745.
- Van Nostrand, W. E., Wagner, S. L., Farrow, J. S., & Cunningham, D. D. (1990b) *J. Biol. Chem.* 265, 9591.
- Van Nostrand, W. E., Schmaier, A. H., Farrow, J. S., Cines, D. B., & Cunningham, D. D. (1991) *Biochem. Biophys. Res. Commun.* 175, 15.
- Van Nostrand, W. E., Schmaier, A. H., & Wagner, S. L. (1992) *Ann. N.Y. Acad. Sci.* 674, 243.
- von dem Borne, P. A. K., Koppelman, S. J., Bouma, B. N., & Meijers, J. C. M. (1994) *Thromb. Haemostas.* 73, 397.
- Walsh, P. N., Mills, D. C. B., & White, J. G. (1977) *Br. J. Haematol.* 36, 281.
- Walsh, P. N., Sinha, D., Kueppers, F., Seaman, F. S., & Blankstein, K. B. (1987) *J. Clin. Invest.* 80, 1578.
- Warn-Cramer, B. J., & Bajaj, S. P. (1985) *Biochem. Biophys. Res. Commun.* 133, 417.

BI9612576